Sensitization of EGFR wild-type non-small cell lung cancer cells to EGFR-tyrosine kinase inhibitor erlotinib.

Judith M Raimbourg, Marie-Pierre M Joalland, Mathilde M Cabart, Ludmilla de Plater, Fanny Bouquet, Ariel Savina, Didier M Decaudin, Jaafar Bennouna, François M Vallette, Lisenn Lalier

HAL Id: inserm-01525974
https://inserm.hal.science/inserm-01525974

Submitted on 22 May 2017

Sensitization of EGFR wild-type non-small cell lung cancer cells to EGFR-Tyrosine Kinase Inhibitor erlotinib.

Judith Raimbourg[1,2,3], Marie-Pierre Joalland[1,2,3], Mathilde Cabart[1,2,4], Ludmilla de Plater[5], Fanny Bouquet[6], Ariel Savina[6], Didier Decaudin[5,7], JaafarBennouna[1,2,3], François M Vallette[1,2,3*] and LisennLalier[1,2,3*]

[1]UMR 1232 INSERM, Nantes, France; [2]Faculty of Medicine, NantesUniversity, Nantes, France; [3]Institut de Cancérologie de l'Ouest, Nantes-Saint Herblain, France; [4]Institut Bergonié, Bordeaux, France; [5]Laboratory of Preclinical Investigation, TranslationalResearchDepartment, Institut Curie, PSL University, Paris, France; [6]Institut Roche, Boulogne-Billancourt, France; [7]Department of MedicalOncology, Institut Curie, Paris, France.

Running title:wtEGFR non-small cell lung cancer sensitization to erlotinib

Keywords: cancer, non-small cell lung cancer, chemotherapy, EGFR,

* correspondance to:LisennLalier, LaBCT INSERM U1232, Institut de Cancérologie de l'Ouest, bd Jacques Monod, 44800 Saint Herblain, lisenn.lalier@univ-nantes.fr; **or to:** François M Vallette, CRCINA INSERM U1232, IRSUN, 8 quai Moncousu, 44007 Nantes Cedex 01, francois.vallette@univ-nantes.fr.

6 figures, 4946 words

Abstract

The benefit of EGFR-TKI in non-small cell lung cancer has been demonstrated in mutant EGFR tumors as first-line treatment but the benefit in wild-type EGFR tumors is marginal as well as restricted to maintenance therapy in pretreated patients. This work aimed at questioning the effects of cisplatin initial treatment on the EGFR pathway in non-small cell lung cancer and the functional consequences *in vitro* and in *in vivo* animal models of Patient-Derived Xenografts (PDX). We establish here that cisplatin pretreatment specifically sensitizes wild-type EGFR expressing cells to erlotinib, contrary to what happens in mutant-EGFR cells and with a blocking EGFR antibody, both *in vitro* and *in vivo*. The sensitization entails the activation of the kinase Src upstream of EGFR, thereafter transactivating EGFR through a ligand-independent activation. We propose a combination of markers which enable to discriminate between the tumors sensitized to erlotinib or not in PDX models, that should be worth testing in patients.These markers might be useful for the selection of patients who would benefit from erlotinib as a maintenance therapy.

Introduction

EGFR is the receptor for epidermal growth factor (EGF) and belongs to the tyrosine kinase receptors (RTK).This transmembrane receptor protein is involved in the fine regulation of epithelial cells proliferation through the extracellular binding of its ligands and the complex cross-talk with several membrane receptors, including the other members of the erbB/HER-family(1). The very subtle regulation is achieved by the multiplicity and redundancy of the ligands and dimerization partners of EGFR(1, 2). The broad field of its downstream signaling pathways also stands for the multiplicity of biological effects induced by EGFR activation(3). Several reports besides revealed a non-canonical, ligand-independent activation (trans-activation) of EGFR(4) in epithelial and non-epithelial cells(5, 6). This points out that the biological role of EGFR oversteps the sole regulation of cell proliferation in response to EGF-like ligands.

EGFR mutation is one of the major driver mutations in non-small cell lung cancer (NSCLC).EGFR tyrosine kinase inhibitors (EGFR-TKI) have constituted a significant advance in the care of patients which tumors harbour a mutated, activated form of EGFR(7). Conversely, the indication of EGFR-TKI in patients with wtEGFR tumor is more debated (8-10). If the absence of efficacy is demonstrated in first-line treatment, pretreated patients could benefit from EGFR-TKI.Aside from the newly arising immune-based therapies, targeted therapies are of high efficiency in the case of oncogenic mutation-driven tumors, even only a small percentage of tumors are concerned so far. Despite much effort was made in order to find out new therapeutic strategies in lung cancer, platinum-based chemotherapy (associated to pemetrexed) remains the backbone therapy in wild-type EGFR non-small cell lung cancer (NSCLC).

The first-line chemotherapy induces drastic modifications of cancer cells, at the non-genetic(11) or genetic levels (12). Such events are susceptible to alter the cell response to the subsequent treatments and underline the need for repeated biopsies along the treatment (13). This can account for the observations made in clinical trials that wild-type EGFR patients benefit from

EGFR-TKI as amaintenance treatment following to platinum-based first-line therapy (8). High-dose cisplatin treatment was shown to induce EGFR activation in lung cancer cell lines(14). Given the fact that cisplatin is the usual first-line chemotherapy for wild-type EGFR NSCLC, we aimed at investigating the consequences of a sublethal cisplatin treatment upon the surviving cells sensitivity to erlotinib, either in wild-type or mutated-EGFR cell lines. We also questioned the effect of long-term cisplatin exposure to sensitized cells and explored the molecular pathways involved. We finally used lung cancer patients derived xenografts (PDX) to challenge the sensitization observed *in vitro* and found out markers of the described sensitization, thereby bringing a new perspective to the use of EGFR-TKI in EGFR wild-type NSCLC.

Materials and methods

Material used

wtEGFR (A549, H358 and H522) and mutant EGFR cell lines (H1650 and H1975) were purchased from the ATCCbetween 2011 and 2012. Cells from an individual frozen stock vial were grown for a maximum of four consecutive months and were monthly tested for Mycoplasma contamination. They were grown and treated by the indicated drugs in 10% fetal bovine serum-containing medium (RPMI 1640, Gibco, ThermoFischer Scientific) unless otherwise stated. The references of the antibodies used were following: membrane EGFR, Santa Cruz #sc-120; membrane Her2, Santa Cruz #sc-23864; membrane Her3, Santa Cruz #sc-71068; phospho-EGFR (Y1068), Cell Signaling Technology #3777; phospho-AKT (S473), Cell Signaling Technology #9271; phospho-ERK1/2 (T202/Y204), Cell Signaling Technology #9101; total EGFR, Cell Signaling Technology #4267; GRB2, BD Biosciences #610112; pTyr100, Cell Signaling Technology #9411; blocking EGFR antibody (225), Invitrogen #MA5-12880; blocking IL6 antibody, R&D Systems #MAB206; control IgG1, RnD Systems #MAB002. PP1 and PP2 inhibitors (15)were purchased from Sigma Aldrich (#P0040 and #P0042). ELISA kits were purchased from R&D Systems and used according to the manufacturer's instructions.

All experiments were repeated three times independently unless otherwise stated and analyzed by Student t-test.

Flow cytometry

Flow cytometry was performed with BD Accuri C6 cytometer. The detection of membrane proteins was performed with intact cells at 4°C with the indicated antibodies diluted in 1% BSA coupled to fluorescent (FITC) secondary antibodies. For the detection of intracellular proteins, cells were fixed by 4% paraformaldehyde, permeabilised by 0.5% saponin and saturated by 5% BSA. Antibodies were diluted in PBS-0.1% saponin-1% BSA and coupled to fluorescent (FITC) secondary antibodies. Non-specific binding of secondary antibodies in every experiment was measured by omitting primary

antibody and the corresponding mean fluorescence was substracted from the signal measured with each primary antibody.

Viability assay

Cells were plated in 6-well plates and treated by the indicated drugs. At the indicated time points, cells were harvested by trypsination and dead/dying cells were detected by To-Pro3 internalization measured by flow cell analysis (BD Accuri C6 cytometer). The results are presented as the mean fluorescence of the overall population (+sd) or as the mean percentage of To-Pro3 positive cells (+sd).

Conditioned medium preparation

Cells were plated in 100mm-dishes and treated by cisplatin (3µM, 48h). Cells were then rinsed and culture medium was replaced by fresh serum-free medium. After 48h, cell supernatant was centrifuged to remove cells fragments and used for the described experiments. Cells were trypsinised and counted to normalize ligand measurements by the cell number.

Proximity Ligation Assay (PLA)

Cells were seeded in 24-well plates onto glass sterile coverslips and allowed to attach overnight. The indicated treatment was applied, then cells were fixed by 4% paraformaldehyde. The labeling with antibodies was realized according to the PLA manufacturer instructions (Duolink, Sigma-Aldrich). Image acquisition was performed with a Zeiss Apotome microscope (Zeiss Axiovert 200-M inverted microscope and AxioVision 4.6 program, Carl Zeiss Gbmh). Data were analyzed by the ImageJ 1.46r software and spots were quantified by the Object 3D Counter plugin.

IC50 measurements

IC50 measurements were calculated according to Chou *et al*.(16) by the MTT method. Briefly, cells were plated in 96-well plates (5000 cells/well) and treated by the indicated drugs or conditioned

media. Cells were incubated with MTT 3h at 37°C, formazan cristae were solubilized in DMSO and optical density (OD) was read at 570nm.

Preclinical PDX models

Four to six week-old Nude mice, bred at Institut Curie, were used. Tumor fragments of 30-50mm^3 were grafted subcutaneously into the interscapular fat pad. When tumors reached a size of about 50-100mm^3, mice were randomly assigned to control or treatment groups. Between 8 and 10 mice per group were included in each experiment. Mice were sacrificed when tumor reached a volume of 2500mm^3. All treatments are detailed in the Results section. Tumor growth was evaluated by measuring with a caliper two perpendicular tumor diameters twice a week. Individual tumor volume, relative tumor volume (RTV) and tumor growth inhibition (TGI) were calculated according to a standard method. Studies have been performed in compliance with protocol and animal housing in accordance with national regulation and international guidelines and under the supervision of authorized investigators. The experimental protocol and animal housing were in accordance with institutional guidelines as put forth by the French Ethical Committee (Agreement C75-05 - 18, France). For all pairwise comparisons based on the proportions of tumors with a particular RTV, a two-tailed Fischer's exact t-test was used. All statistical tests were realized bilaterally calculating two-tailed p-values.

RT and qPCR

Total RNA was isolated from cell pellets or from frozen PDX pieces using the RNeasy MiniKit (Qiagen) following the manufacturer's instructions with DNase I treatment. After RNA quantification by spectrophotometry (BioSpectrometer, Eppendorf, France), 1µg RNA was reverse-transcribed with Quantiscript Reverse Transcriptase (Qiagen, France) for cDNA synthesis. Quantitative real-time PCR assays were performed and monitored in technical duplicate using a Rotor-Gene Q PCR system (Qiagen, France). Data were normalised by three housekeeping genes (RPLP0, Actin and GAPDH)and expressed as fold change versus control conditions (non-treated cells or control mice). Primers used

were purchased from Qiagen and validated by the supplier (QuantiTect primers : IFIT1 QT00201012, IFI27 QT00099274, IL6 QT00083720, RPLP0 QT00075012, Actin QT01680476, GAPDH QT00079247).

PCA analysis

PCA analysis (Pearson's correlation) was performed from the data described in Table S1 using XLSTAT v2016.03 software (Addinsoft 2010).

Results

Cisplatin primes EGFR wild-type cells toerlotinib through the activation of EGFR pathway.

We worked with three EGFR wild-type (wtEGFR) cell lines (namely A549, H358 and H522) and with two mutant EGFR (mutEGFR) cell lines (H1650 and H1975, respectively exhibiting A746-A750 deletion and L858R-T790M mutations). We first measured the membrane expression of EGFR, Her2 and Her3 in the different cell lines (figure 1A). Most of the cell lines significantly expressed EGFR, except from H522 cells. H522 cells essentially expressed HER2; of note, total EGFR expression in H522 cells was very faint,either by cytometry or by western blot analyses, as reported by others (17). Her3 membrane expression was hardly detected in the cell lines used. Given the previously reported activation of EGFR pathway induced by cisplatin(18, 19), we measuredEGFR phosphorylation following a non-lethal cisplatin treatmentin wild type-EGFR cells and observed that the phosphorylation raised during the 48 hour-cisplatin treatment, together with the subsequent activation of EGFR downstream kinases ERK and AKT to a lesser extent (figure 1B). We wondered if the activation of EGFR pathway observed was associated to a change in the cells sensitivity to EGFR tyrosine kinase inhibition. We sequentially treated the cells with a sublethal amount of cisplatin for 48 hours, then with various erlotinib amounts for 72 hours, according to their respective IC50 (figure S1-A). In the cell lines expressing a significant amount of wtEGFR (namely A549 and H358 cells), cisplatin actually primed the cells to erlotinib-induced cell death (figure 1C and figure S1-B).Erlotinib actually reversed the phosphorylation of ERK kinase induced by cisplatin in wtEGFR-expressing cells (figure S2-A and B). By contrast, no decrease in the IC50 to erlotinib of mutEGFR-expressing cells was observed in cisplatin-treated cells versus naive cells, rather a significant raise in cisplatin-treated H1975 cells IC50 (figure S2-C). Of note, the treatment schedule came out as crucial, since concurrent cisplatin-erlotinib treatment did not enhance the wtEGFR cells response to erlotinib (figure S2-D). Cisplatin treatment thus induced a priming event to the subsequent erlotinib treatment. Smith *et al.*(20)established a correlation between EGFR-GRB2 complexes detection and the response to EGFR

inhibitors. We actually confirmed that cisplatin pretreatment significantly up-regulated the amount of EGFR-GRB2 interactions detected by the PLA technique in wtEGFR cells (figure 1D and S2-E).

EGFR is activated in cisplatin-resistant cells.

We generated a cisplatin-resistant cell line derived from A549 cells by constant exposure to 3μM cisplatin. After a few weeks, cells began to proliferate and could be passaged and subcultured in the presence of cisplatin. We objectified the resistance to cisplatin of these cells, named A549cis3, by measuring their IC50 to cisplatin (figure 2A). These A549cis3 cells revealed more sensitive to erlotinib than their parent cells (figure 2B, left) and exhibited a higher level of phosphorylated EGFR (figure 2B, right), similar to that measured in the cells treated by cisplatin for 48h. We noticed that A549cis3 cells grew more slowly than A549 parental cells and had a different morphology (figure 2C). Thesephenotypic modifications are sometimes reported when epithelial-to-mesenchymal transition (EMT) occurs. We therefore challenged this hypothesis by measuring the expression of vimentin and E-cadherin in the cells, and we measured no significant change in A549cis3 cells versus the A549 parental cells (figure 2D) indicating no EMT in A549cis3 cells.

Cisplatin induces EGFR activation in wtEGFR cells through the secretion of an activator, distinct from EGFR ligands.

EGFR is classically activated through the binding of its ligands and consequent dimerization responsible for its autophosphorylation. We first challenged the ability of cisplatin-treated cells to increase the sensibility of wtEGFR naive cells to erlotinib. We prepared conditioned media (CM) from A549 cells either treated by cisplatin (3μM, 48h) or not and from the resistant A549cis3 cells. Naive A549 cells were incubated overnight with the conditioned media and then treated by erlotinib. The conditioned media from cisplatin-treated and cisplatin-resistant cells decreased the cells resistance to erlotinib (figure 3A), indicating that a secreted factor is implicated in the cisplatin-induced sensitization to erlotinib. To objectify EGFR activation, we measured EGFR phosphorylation by theDuolink technique. We actually observed that cisplatin-treated cells secrete a soluble factor

responsible for EGFR phosphorylation (figure 3B). We measured the secretion of EGFR ligands and of some known regulators of EGFR activation (namely PGE2 and HGF)by cisplatin-treatedwtEGFR cells.Amphiregulin secretion was increased by cisplatin treatment in all the tested cell lines (figure 3C, left graph). TGFα secretion was induced in two cell lines except from the A549 cells (figure 3C, middle graph) while PGE2 secretion was only induced in A549 conditioned medium (figure 3C, right graph). We made several attempts to establish the role of these secreted molecules in the sensitization to erlotinib observed. As cisplatin-treated A549 CM could sensitize A549 cells to erlotinib, we treated naive A549 cells with recombinant amphiregulin, PGE2 or the combination of both, at the concentrations measured in the conditioned media, but the sensitivity of the treated cells to erlotinib was not modified (figure S3-A).We tested the ability of various CM obtained from control and cisplatin-treated cell lines to sensitize A549 cells to erlotinib related to the evolution of the same EGFR regulators concentrations as in figure 3C. As summarized in figure 3D, these experiments could not shed the light on any regulator or combination of regulators. In order to conclude on the direct activation of EGFR by a secreted molecule induced by cisplatin, we questioned the sensitivity of the naive and cisplatin-treated wtEGFR cells to a blocking EGFR antibody (analog to the anti-EGFR drug cetuximab). As indicated in figure 3E and supplementary figure S3-B, the blocking EGFR antibody induced an obvious cell death in wtEGFR cells and cisplatin pretreatment abrogated the cells sensitivity to EGFR antibody. This definitely ruled out the possibilitythat the observed activation of EGFR results from the binding of any ligand, suggesting a ligand-independent activation of EGFR, whilst related to a secreted factor.

The sensitization to erlotinib induced by cisplatin pretreatment implies the activation of the Src kinase.

Considering the transactivating role played by the Src-family kinases in EGFR pathway(21), we questioned the role played by Src (or SFKs) in the activation of EGFR induced by cisplatin. We first induced Src pharmacological inhibition during the cisplatin pretreatment step. The addition of PP1

(Src inhibitor-1, figure S4-A) to wtEGFR cells during the cisplatin pretreatment significantly inhibited the subsequenterlotinib-induced cell death (figure 4A). Of note, similar results were observed with another Src inhibitor (PP2, figure S4-B). We have previously shown that cisplatin induced no sensitization to erlotinib in the EGFR-mutated H1975 cell line (figure S2-C). We thus compared the effect of Src inhibition during cisplatin pretreatment in both cell lines. No significant cell death was induced by erlotinib in cisplatin-pretreated H1975 cells, contrary to A549 cells (figure 4B, upper graph). Additionally and contrary to what happened in wtEGFR cells, Src inhibition during the initial cisplatin treatementrevealed asignificant cell death induced by erlotinib in H1975 cells (figure 4B, lower graph). This further substantiates the different responses of wtEGFR and mutEGFR cells to the sequential treatment cisplatin-erlotinib (figure 1C and figure S2-C). We next measured EGFR phosphorylation in wtEGFR cells either treated by cisplatin or by the combination cisplatin+PP1. We observed that Src inhibition counteracted the phosphorylation of EGFR induced by cisplatin (figure 4Cand figure S4-C). Given the role played by IL6 in the ligand-independent activation of EGFR (22), we measured the secretion of IL6 induced by cisplatin in wtEGFR A549 cells. As shown on figure 4D, IL6 secretion was significantly increased after a 48 hour cisplatin treatment. We therefore added neutralizing IL6 antibody in the culture medium of A549 cells treated by the sequential treatment cisplatin / erlotinib. IL6 counteraction significantly reduced the priming of wtEGFR cells to erlotinibby cisplatin (figure 4E), demonstrating that IL6 is involved in this sensitization.

Cisplatin injection can sensitize wtEGFR patients-derived xenografts to erlotinib*in vivo*.

We next investigated the capacity of cisplatin initial treatment to enhance the response of wtEGFR*tumors to erlotinib*in vivo*. We used a set of four PDXs (patient-derived xenografts) (LCF-04, LCF-09, IC14-LC16 and IC8-LC10), obtained from human non-small cell lung cancer (NSCLC) pieces xenografted to Swiss Nude mice. The use of PDXs for preclinical studies was shown to better reflect the phenotype and heterogeneity of human lung cancer tumors than cell lines xenografts(23-25).The histological type of PDX was confirmed and compared to the initial tumors. Tumors were classified as

adenocarcinomas and expressed wild-type EGFR, KRAS, BRAF and PI3K. Mice were randomly assigned to four groups since tumors reached an initial volume ranged between 50 and 100mm^3. The "control" group received no treatment; the "cisplatin" group received an intraperitoneal injection of cisplatin at day 1 (6mg/kg); the "erlotinib" group was orally treated by erlotinib(50mg/kg) 5 days out of 7 from day 7 to the mice sacrifice; the "cisplatin/erlotinib" group was treated by both drugs as described above. Tumor growth was measured twice a week and represented on the graphs in figure 5 as mean relative tumor volume in each group +/- SD. In comparison to each monotherapy, *i.e.* cisplatin or erlotinib, tumor growth was significantly inhibited by the sequential treatment in three out of four models with variable efficiency, whereas no benefit was observed in tumor D (IC8-LC10) either at early or late time points.Of note, when tumors were allowed to grow for a longer time (figure S5), the initial sensitization to erlotinib tended to disappear in two PDX models.Differences are observed in tumor growth rates and response to each drug or drug combination, which is consistent with the heterogeneity of lung tumors phenotype. These results suggest that cisplatin may actually enhance the response of some human NSCLC tumors to erlotinib*in vivo* and require the identification of these tumors by the definition of a predictive marker.

IL6, IFIT1 and IFI27 measurement can discriminate between responding and non-respondingwtEGFR tumors.

We have demonstrated the role played by IL6 in the ligand-independent activation of EGFR induced by cisplatin. Ligand-independent activation of EGFR is correlated to IFIT1 and IFI27 transcription in glioma (26). We therefore measured the expression induction of IL6, IFIT1 and IFI27 in cisplatin-treated (A549 + cisp) and cisplatin-resistant (A549cis3) A549 cells. The transcription of all three markers was increased in cisplatin-treated and cisplatin-resistant cells (figure 6A), in a time-dependent manner for the short-term treatment (figure S6-A). These three potential markers were challenged for their fitting to the sensitization of wtEGFRtumors to erlotinib*in vivo* by the use of the PDX models described above. PDXs A, B and D (figure 5) were grafted to Swiss Nude mice. Mice were

treated by cisplatin at day 1 after randomization. Mice were sacrificed at day 4, 8 and 18and tumors were excised and frozen. A group of control, non-treated mice was sacrificed at day 4.mRNA were extracted from the tumors and analyzed for the expression of IL6, IFIT1 and IFI27. Figure 6B shows the cumulative expression of the three markers for each PDX in the four groups of mice. As indicated on the graphs, the cumulative expression exceeds the value of 5 for the PDXs A and B (which were sensitized by cisplatin to erlotinib) whereas the cumulative value remains below in the PDX D,resistant to the sequential treatment. A principal component analysis (PCA, Pearson's correlation) was performed with the three quantitative variables (IL6, IFIT1 and IFI27) and two qualitative variables added, namely the time post-cisplatin treatment and the sensitization to erlotinib of the tumor (tumors A and B: responding, tumor D: non responding) (see table S1 for details). As represented in figure 6C and figure S6, these markers could discriminate between responding and non-responding PDXs. The time point day-8 seems to divert from the other time points. We therefore repeated the same PCA with the measurement made from the PDXs at day-8 and the analysis efficiently discriminated between responding and non-responding PDXs (figure S6-B) (98.37%). As described in figure S7, at day 8, only tumors from the PDX D group can be found in the Treatment-NT confidence ellipse, whereas responding tumors significantly diverge from this ellipse at day 8.

Discussion

The aim of our study was to increase understanding of the modifications induced in NSLCL cells by a cisplatin sublethal treatment towards EGFR pathway. We provide here evidence of a ligand-independent, Src-mediated activation of EGFR induced by cisplatin treatment in NSCLC cells expressing wild-type EGFR. This activation results in a sensitization of wtEGFR cells to erlotinib, an EGFR-TKI.This increase in erlotinib efficiency is reproduced *in vivo* in PDX models, which is reported for the first time to our knowledge. Some previous reports have shown the ability of chemotherapy, including cisplatin, to induce EGFR activation, in several cell types (14, 27-29) but the functional consequences regarding the cells sensitivity to EGFR inhibition are less clear. Surprisingly, depending on the model considered, EGFR activation either promoted cell survival and tumor growth (14)or sometimes cell death (27). This activation sometimes functionally came out as an increased sensitivity to EGFR inhibitors, either EGFR-TKI or EGFR blocking antibody (29), sometimes not (19). The signaling pathways leading to EGFR activation as well as pathways activated by EGFR phosphorylation are extremely various. These many signaling options could explain thediscrepancies between *in vitro* or clinical reports studying the interplay between chemotherapy and EGFR inhibition. The sequence of events we describe here, leading to the increase in erlotinib efficiency, may be specific from platinum-based priming. This will be the subject of further investigation.

The observations we report here are in agreement with the conclusions of the clinical study SATURN that established the benefit of erlotinib as maintenance therapy in patients with EGFR-positive NSCLC after four cycles of platinum-doublet chemotherapy (8). A more recent study reevaluated the results of the SATURN and BR.21 trials with a focus on wtEGFR patients and confirmed the benefit of erlotinibafter initial platinum doublet therapy in these patients (30).Recently, the IUNO clinical trial comparing the benefit of erlotinib as maintenance treatment versus as second line therapy in wtEGFR patients failed at demonstrating any benefit of erlotinib in the cohort with either therapeutic schedule (31).Clinical studies suggest that erlotinib maintenance

could be more efficient in tumor controlled by the initial platinum-based therapy(32).We have established that cisplatin-resistant cells, arisen from constant exposure of sensible cells to cisplatin, exhibited the same pattern of EGFR activation and erlotinib sensitivity as short-term treated cells. This suggests that some patients could benefit from erlotinib maintenance even if tumor escapes from platinum-based chemotherapy, providing the markers of sensitization are expressed. The increased sensitivity of chemotherapy-resistant cells to EGFRinhibition has also been observed in other cell types, suggesting that this sensitization may not solely interest lung cancer cells and cisplatin (28). Of note, Rho *et al.* observed that the generation of cisplatin-resistant cells by discontinued exposure of cells to increasing concentration followed by drug vacancy did not alter the cells sensitivity to EGFR-TKIs (33). This is consistent with our findings that erlotinib must be given short after cisplatin treatment, whatever the duration of cisplatin exposure. The observations made in our PDX models also suggest that erlotinib benefit is maximal at early time after cisplatin treatment. Repeated cisplatin injections may be of interest to restore erlotinib sensitization when tumor escape happens and could be assayed. This hypothesis is substantiated by a very recent meta-analysis of randomized clinical trials suggesting that the addition of intercalated EGFR-TKI to chemotherapy could be of interest in NSCLC (34). An *in vitro* study demonstrated however that EGFR-TKI tolerance results from reversible, epigenetic cell phenotype modifications (11). These modifications also result in a decreased sensitivity to cisplatin, suggesting that erlotinib-resistant tumors should be either submitted to a transient drug vacancy or to an HDAC inhibitor before cisplatin should be repeated. All together, these studies further reinforce the need of markers to identify the tumors susceptible to respond to EGFR-TKI and the optimal moment when they should be introduced in the therapeutic schedule.

This point, namely the utmost importance of the kinetics of the therapeutic schedule, underlines the major difference between the epigenetic, inheritable mechanism of EGFR-TKI tolerance described by Sharma *et al.*(11) and the mechanism of cisplatin resistance observed in our model, the former rendering the cells resistant to cisplatin and the latter rendering the cells sensitive

to EGFR-TKI by the activation of a specific pathway. The results we report herecompared to those reported by Sharma *et al.*(11)point out the importance of the sequence of cisplatin and erlotinib therapies. The initial cisplatin treatment is required for EGFR activation prior to erlotinib introduction, whereas initial EGFR-TKI treatment might favor the resistance of surviving cells to cisplatin. The observation that erlotinib combination with concurrent cisplatin showed no clinical benefit (9) also corroborates our *in vitro* data and the requirement of the sequential treatment. It also became quite clear, both *invitro* and *in vivo*, that EGFR inhibition impairs the efficiency of chemotherapy when administrated first (35). Tumor cells drastically evolve from the initial biopsy-based analyses to the therapy-modified phenotype at the time of maintenance, underlining the needforphenotypic reevaluationafter the first-line therapy to optimize the therapeutic strategy(13).What we show here is that the initial cisplatin treatment induces a cell phenotype modification, linked to Src-dependent and ligand-independent EGFR activation. In this modified cells, EGFR tyrosine kinase function is required to cell survival, since erlotinib then induces cell death.

The activation of EGFR by cisplatin pretreatment we describe here is ligand-independent. This might explain the poor predictive value (even the inverse correlation) of serum EGFR ligands measurements towards EGFR-TKI efficiency sometimes reported(36, 37). Chakraborty *et al.*(26)have demonstrated in glioblastoma that ligand-induced and ligand-independent activation of EGFR are distinct and even compete with each other. They report that ligand-independent activation of EGFR signals through the activation of interferon regulatory factor 3 (IRF3) and the up-regulation of its targets IFIT1 and IFI27. Of note, we also observed IFIT1 upregulation in short-term and long-term treated cells, with sublethal amounts of cisplatinfor A549 cells (3μM), consistent with patients serum concentration; as for death-inducing cisplatin treatment (100μM), Galluzzi*et al* (38)reported the upregulation of two related interferon regulatory factors (IRF7 and IRF5), suggesting that type I interferon pathway may be implicated in cisplatin-induced cell modifications. Our data suggest that IFIT1 and IFI27 induction assessment, together with that of IL6, may enable the discrimination between the tumors sensitized to erlotinibby cisplatin pretreatment or not. The correlation between

these markers and the efficiency of erlotinib maintenance should be addressed in wtEGFR lung cancer patients after a first-line cisplatin treatment.

Similar to what was demonstrated in glioblastoma (26), we show here that cisplatin pretreatment in NSCLC simultaneously renders the cells more sensitive to EGFR-TKI and more resistant to EGFR blocking antibody. It is thus of high importance to consider that EGFR-TKI and EGFR blocking antibody are not redundant and substitutable therapeutic strategies. The former should predominantly target ligand-independent EGFR signaling whereas the latter should only inhibit the ligand-induced signaling. Combining both EGFR targeting strategies may thus enhance tumor response in some models. Some fruitful attempts were reported*in vitro* in several models (39-41) or in clinical trials in lung cancer(42) or in colorectal cancer (43).

Finally, it is noteworthy that both cell lines sensitized to erlotinib by cisplatin we used in this study express mutated KRAS, whereas all the PDX models we worked with express wild-type KRAS. In the SATURN cohort of patients, KRAS mutation was a significant prognostic factor for poor response to erlotinib(44).KRAS nevertheless does not appear as a major determinant for the mechanism we describe. This KRAS-independent signaling induced by cisplatin pretreatment is consistent with the activation of ligand-independent EGFR pathway, rather implicating TBK1-IRF3 complex (4). A549 cells express G12S-KRAS and H358 cells express G12C-KRAS. Singh *et al.*(45) have established that A549 cells were independent from KRAS for their survival, since KRAS knock-down had no impact on cell growth or on downstream kinases (ERK and AKT) phosphorylation. Besides, the constitutive activation of downstream effectors ERK and AKT by G12C-KRAS was the same as wild-type KRAS(46). The regulation of ERK and AKT phosphorylation in our KRAS mutated cell lines would thus not involve KRAS. The activation induced by cisplatin might rather be the consequence of Src activation. KRAS mutation should therefore not be an absolute exclusion criterion for EGFR-TKI therapy, in case of ligand-independent activation of EGFR.This suggestion is supported by the observation made in metastatic colon cancer:whereas anti-EGFR antibodies proved to be effective in colorectal cancer

excluding the KRAS mutated tumors, the GERCOR DREAM study shows the benefit oferlotinibin maintenance therapy in KRAS mutated colon cancer in combination with angiogenesis inhibition after induction chemotherapy (47).

In conclusion, this work highlights the occurrence of ligand-independent EGFR activation in cisplatin-treated wtEGFR NSCLC. Similar to what happens in glioblastoma, this pathway competes with ligand-induced EGFR signaling(4, 26), involving plasma membrane EGFR. This could support the fact that some wtEGFR patients may benefit from EGFR-TKI as maintenance therapy when given immediately following to platinum-based therapy. The balance between both activation pathways can account for the reported additive effect of EGFR-TKI and EGFR antibody strategies in some tumors. To achieve this optimization of EGFR-TKI, the validation of ligand-independent EGFR activation markers in NSCLC cohorts is required and will be the subject of further development.

Acknowledgements

References

1.   Ciardiello F, Tortora G. EGFR antagonists in cancer treatment. N Engl J Med. 2008;358(11):1160-74.
2.   Roepstorff K, Grandal MV, Henriksen L, Knudsen SL, Lerdrup M, Grovdal L, et al. Differential effects of EGFR ligands on endocytic sorting of the receptor. Traffic. 2009;10(8):1115-27.
3.   Huang PH, Xu AM, White FM. Oncogenic EGFR signaling networks in glioma. Sci Signal. 2009;2(87):re6.
4.   Guo G, Gong K, Wohlfeld B, Hatanpaa KJ, Zhao D, Habib AA. Ligand-Independent EGFR Signaling. Cancer Res. 2015;75(17):3436-41.
5.   Hardbower DM, Singh K, Asim M, Verriere TG, Olivares-Villagomez D, Barry DP, et al. EGFR regulates macrophage activation and function in bacterial infection. The Journal of clinical investigation. 2016;126(9):3296-312.
6.   Lu N, Wang L, Cao H, Liu L, Van Kaer L, Washington MK, et al. Activation of the epidermal growth factor receptor in macrophages regulates cytokine production and experimental colitis. Journal of immunology. 2014;192(3):1013-23.
7.   Lynch TJ. Predictive tests for EGFR inhibitors. Clin Adv Hematol Oncol. 2005;3(9):678-9.
8.   Cappuzzo F, Ciuleanu T, Stelmakh L, Cicenas S, Szczesna A, Juhasz E, et al. Erlotinib as maintenance treatment in advanced non-small-cell lung cancer: a multicentre, randomised, placebo-controlled phase 3 study. Lancet Oncol. 2010;11(6):521-9.
9.   Gatzemeier U, Pluzanska A, Szczesna A, Kaukel E, Roubec J, De Rosa F, et al. Phase III study of erlotinib in combination with cisplatin and gemcitabine in advanced non-small-cell lung cancer: the Tarceva Lung Cancer Investigation Trial. J Clin Oncol. 2007;25(12):1545-52.
10.   Zhao N, Zhang XC, Yan HH, Yang JJ, Wu YL. Efficacy of epidermal growth factor receptor inhibitors versus chemotherapy as second-line treatment in advanced non-small-cell lung cancer with wild-type EGFR: a meta-analysis of randomized controlled clinical trials. Lung Cancer. 2014;85(1):66-73.
11.   Sharma SV, Lee DY, Li B, Quinlan MP, Takahashi F, Maheswaran S, et al. A chromatin-mediated reversible drug-tolerant state in cancer cell subpopulations. Cell. 2010;141(1):69-80.
12.   Engelman JA, Zejnullahu K, Mitsudomi T, Song Y, Hyland C, Park JO, et al. MET amplification leads to gefitinib resistance in lung cancer by activating ERBB3 signaling. Science. 2007;316(5827):1039-43.
13.   Politi K, Herbst RS. Lung cancer in the era of precision medicine. Clin Cancer Res. 2015;21(10):2213-20.
14.   Yoshida T, Okamoto I, Iwasa T, Fukuoka M, Nakagawa K. The anti-EGFR monoclonal antibody blocks cisplatin-induced activation of EGFR signaling mediated by HB-EGF. FEBS letters. 2008;582(30):4125-30.
15.   Hanke JH, Gardner JP, Dow RL, Changelian PS, Brissette WH, Weringer EJ, et al. Discovery of a novel, potent, and Src family-selective tyrosine kinase inhibitor. Study of Lck- and FynT-dependent T cell activation. The Journal of biological chemistry. 1996;271(2):695-701.
16.   Chou TC. Theoretical basis, experimental design, and computerized simulation of synergism and antagonism in drug combination studies. Pharmacological reviews. 2006;58(3):621-81.
17.   Engelman JA, Janne PA, Mermel C, Pearlberg J, Mukohara T, Fleet C, et al. ErbB-3 mediates phosphoinositide 3-kinase activity in gefitinib-sensitive non-small cell lung cancer cell lines. Proceedings of the National Academy of Sciences of the United States of America. 2005;102(10):3788-93.
18.   Ametller E, Garcia-Recio S, Pastor-Arroyo EM, Callejo G, Carbo N, Gascon P, et al. Differential regulation of MMP7 in colon cancer cells resistant and sensitive to oxaliplatin-induced cell death. Cancer Biol Ther. 2011;11(1):4-13.
19.   Van Schaeybroeck S, Kyula J, Kelly DM, Karaiskou-McCaul A, Stokesberry SA, Van Cutsem E, et al. Chemotherapy-induced epidermal growth factor receptor activation determines response to

combined gefitinib/chemotherapy treatment in non-small cell lung cancer cells. Molecular cancer therapeutics. 2006;5(5):1154-65.

20. Smith MA, Hall R, Fisher K, Haake SM, Khalil F, Schabath MB, et al. Annotation of human cancers with EGFR signaling-associated protein complexes using proximity ligation assays. Sci Signal. 2015;8(359):ra4.

21. Kopetz S. Targeting SRC and epidermal growth factor receptor in colorectal cancer: rationale and progress into the clinic. Gastrointest Cancer Res. 2007;1(4 Suppl 2):S37-41.

22. Inda MM, Bonavia R, Mukasa A, Narita Y, Sah DW, Vandenberg S, et al. Tumor heterogeneity is an active process maintained by a mutant EGFR-induced cytokine circuit in glioblastoma. Genes & development. 2010;24(16):1731-45.

23. Decaudin D. Primary human tumor xenografted models ('tumorgrafts') for good management of patients with cancer. Anti-cancer drugs. 2011;22(9):827-41.

24. Stewart EL, Mascaux C, Pham NA, Sakashita S, Sykes J, Kim L, et al. Clinical Utility of Patient-Derived Xenografts to Determine Biomarkers of Prognosis and Map Resistance Pathways in EGFR-Mutant Lung Adenocarcinoma. J Clin Oncol. 2015;33(22):2472-80.

25. Gao H, Korn JM, Ferretti S, Monahan JE, Wang Y, Singh M, et al. High-throughput screening using patient-derived tumor xenografts to predict clinical trial drug response. Nature medicine. 2015;21(11):1318-25.

26. Chakraborty S, Li L, Puliyappadamba VT, Guo G, Hatanpaa KJ, Mickey B, et al. Constitutive and ligand-induced EGFR signalling triggers distinct and mutually exclusive downstream signalling networks. Nature communications. 2014;5:5811.

27. Arany I, Megyesi JK, Kaneto H, Price PM, Safirstein RL. Cisplatin-induced cell death is EGFR/src/ERK signaling dependent in mouse proximal tubule cells. American journal of physiology Renal physiology. 2004;287(3):F543-9.

28. Dai Q, Ling YH, Lia M, Zou YY, Kroog G, Iwata KK, et al. Enhanced sensitivity to the HER1/epidermal growth factor receptor tyrosine kinase inhibitor erlotinib hydrochloride in chemotherapy-resistant tumor cell lines. Clin Cancer Res. 2005;11(4):1572-8.

29. Kwon J, Yoon HJ, Kim JH, Lee TS, Song IH, Lee HW, et al. Cetuximab inhibits cisplatin-induced activation of EGFR signaling in esophageal squamous cell carcinoma. Oncology reports. 2014;32(3):1188-92.

30. Osarogiagbon RU, Cappuzzo F, Ciuleanu T, Leon L, Klughammer B. Erlotinib therapy after initial platinum doublet therapy in patients with EGFR wild type non-small cell lung cancer: results of a combined patient-level analysis of the NCIC CTG BR.21 and SATURN trials. Translational lung cancer research. 2015;4(4):465-74.

31. Cicenas S, Geater SL, Petrov P, Hotko Y, Hooper G, Xia F, et al. Maintenance erlotinib versus erlotinib at disease progression in patients with advanced non-small-cell lung cancer who have not progressed following platinum-based chemotherapy (IUNO study). Lung Cancer. 2016;102:30-7.

32. Coudert B, Ciuleanu T, Park K, Wu YL, Giaccone G, Brugger W, et al. Survival benefit with erlotinib maintenance therapy in patients with advanced non-small-cell lung cancer (NSCLC) according to response to first-line chemotherapy. Ann Oncol. 2012;23(2):388-94.

33. Rho JK, Choi YJ, Choi YR, Kim SY, Choi SJ, Choi CM, et al. The effect of acquired cisplatin resistance on sensitivity to EGFR tyrosine kinase inhibitors in EGFR mutant lung cancer cells. Oncology research. 2011;19(10-11):471-8.

34. La Salvia A, Rossi A, Galetta D, Gobbini E, De Luca E, Novello S, et al. Intercalated Chemotherapy and Epidermal Growth Factor Receptor Inhibitors for Patients With Advanced Non-Small-cell Lung Cancer: A Systematic Review and Meta-analysis. Clinical lung cancer. 2017;18(1):23-33 e1.

35. Janku F, Stewart DJ, Kurzrock R. Targeted therapy in non-small-cell lung cancer--is it becoming a reality? Nature reviews Clinical oncology. 2010;7(7):401-14.

36. Addison CL, Ding K, Zhao H, Le Maitre A, Goss GD, Seymour L, et al. Plasma transforming growth factor alpha and amphiregulin protein levels in NCIC Clinical Trials Group BR.21. J Clin Oncol. 2010;28(36):5247-56.

37.   Ishikawa N, Daigo Y, Takano A, Taniwaki M, Kato T, Hayama S, et al. Increases of amphiregulin and transforming growth factor-alpha in serum as predictors of poor response to gefitinib among patients with advanced non-small cell lung cancers. Cancer Res. 2005;65(20):9176-84.

38.   Galluzzi L, Vitale I, Senovilla L, Eisenberg T, Carmona-Gutierrez D, Vacchelli E, et al. Independent transcriptional reprogramming and apoptosis induction by cisplatin. Cell cycle. 2012;11(18):3472-80.

39.   Huang S, Armstrong EA, Benavente S, Chinnaiyan P, Harari PM. Dual-agent molecular targeting of the epidermal growth factor receptor (EGFR): combining anti-EGFR antibody with tyrosine kinase inhibitor. Cancer Res. 2004;64(15):5355-62.

40.   Matar P, Rojo F, Cassia R, Moreno-Bueno G, Di Cosimo S, Tabernero J, et al. Combined epidermal growth factor receptor targeting with the tyrosine kinase inhibitor gefitinib (ZD1839) and the monoclonal antibody cetuximab (IMC-C225): superiority over single-agent receptor targeting. Clin Cancer Res. 2004;10(19):6487-501.

41.   Regales L, Gong Y, Shen R, de Stanchina E, Vivanco I, Goel A, et al. Dual targeting of EGFR can overcome a major drug resistance mutation in mouse models of EGFR mutant lung cancer. The Journal of clinical investigation. 2009;119(10):3000-10.

42.   Janjigian YY, Smit EF, Groen HJ, Horn L, Gettinger S, Camidge DR, et al. Dual inhibition of EGFR with afatinib and cetuximab in kinase inhibitor-resistant EGFR-mutant lung cancer with and without T790M mutations. Cancer discovery. 2014;4(9):1036-45.

43.   Weickhardt AJ, Price TJ, Chong G, Gebski V, Pavlakis N, Johns TG, et al. Dual targeting of the epidermal growth factor receptor using the combination of cetuximab and erlotinib: preclinical evaluation and results of the phase II DUX study in chemotherapy-refractory, advanced colorectal cancer. J Clin Oncol. 2012;30(13):1505-12.

44.   Brugger W, Triller N, Blasinska-Morawiec M, Curescu S, Sakalauskas R, Manikhas GM, et al. Prospective molecular marker analyses of EGFR and KRAS from a randomized, placebo-controlled study of erlotinib maintenance therapy in advanced non-small-cell lung cancer. J Clin Oncol. 2011;29(31):4113-20.

45.   Singh A, Greninger P, Rhodes D, Koopman L, Violette S, Bardeesy N, et al. A gene expression signature associated with "K-Ras addiction" reveals regulators of EMT and tumor cell survival. Cancer Cell. 2009;15(6):489-500.

46.   Ihle NT, Byers LA, Kim ES, Saintigny P, Lee JJ, Blumenschein GR, et al. Effect of KRAS oncogene substitutions on protein behavior: implications for signaling and clinical outcome. Journal of the National Cancer Institute. 2012;104(3):228-39.

47.   Tournigand C, Chibaudel B, Samson B, Scheithauer W, Vernerey D, Mesange P, et al. Bevacizumab with or without erlotinib as maintenance therapy in patients with metastatic colorectal cancer (GERCOR DREAM; OPTIMOX3): a randomised, open-label, phase 3 trial. Lancet Oncol. 2015;16(15):1493-505.

Legends of figures

Figure 1: A, The membrane expression of EGFR, Her2 and Her3 was measured by flow cytometry in the five cell lines used in the study. Data shown are the mean + SD from 3 independent experiments. B, A549 (upper graph) and H358 (lower graph) cells were treated by cisplatin 3µM 48h (cisp). Cells were then fixed and incubated with pEGFR (pY1068), pAKT (pS473) or pERK (pT202-pY204) antibodies. Fluorescence was measured by flow cytometry. Data shown are the mean + SD from 3 independent experiments. **: p<0.01 Student t-test. C, A549 cells were treated by cisplatin 3µM 48h then by erlotinib 15 or 30µM for 72h. Dead cells were stained by To-Pro3 and detected by flow cytometry. The upper graph shows the mean fluorescence (+SD) of the overall population and the lower graph indicates the percentage (+SD) of To-Pro3 positive cells. The graph shown is representative of 3 independent experiments. **: p<0.01 Student t-test. D, Cells were treated by cisplatin 3µM 48h, fixed and incubated with EGFR and GRB2 antibodies. EGFR-GRB2 dimers were detected by PLA. Apotome images were analyzed by ImageJ and the number of foci per cell was represented on the graphs below. Each graph shown is representative of 3 independent experiments.
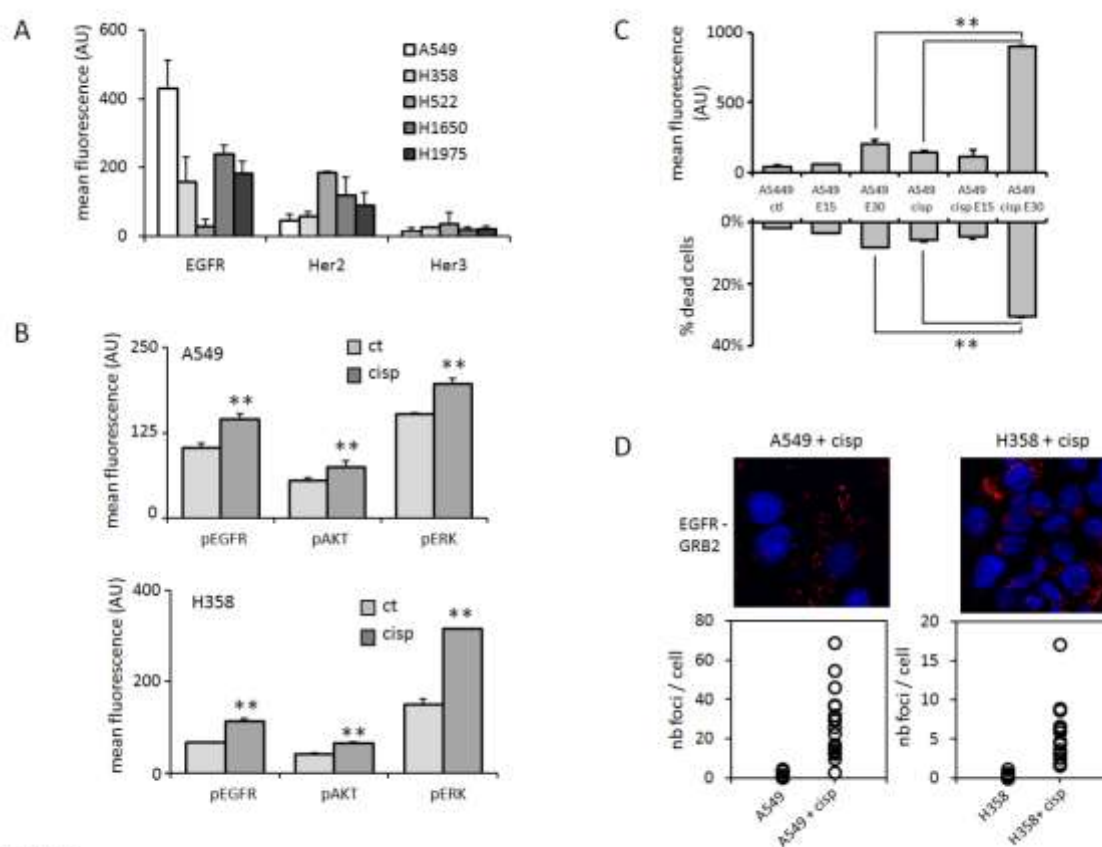

Figure 1

Figure 2: A, A549 and A549cis3 cells were treated by a range of increasing cisplatin concentrations for 48h and IC50 was calculated as described by Chou et al. (16) by MTT assay. Data shown are the mean + SD from 3 independent experiments.**: $p < 0.01$ Student t-test. B, (left) IC50 to erlotinib 72h was calculated for A549 and A549cis3 cells as in (A); (right) EGFR phosphorylation was measured in A549 and A549cis3 cells as described in figure 1(B).*: $p < 0.05$ **: $p < 0.01$ Student t-test. C, The morphology of subconfluent A549 and A549cis3 cells is shown; the fields shown are representative of the global population of each cell type. D, Vimentin and cadherin mRNA expression was measured by RT-PCR and expressed as fold change in A549cis3 cells versus A549 cells. The graph shows the mean + SD from 5 independent experiments.
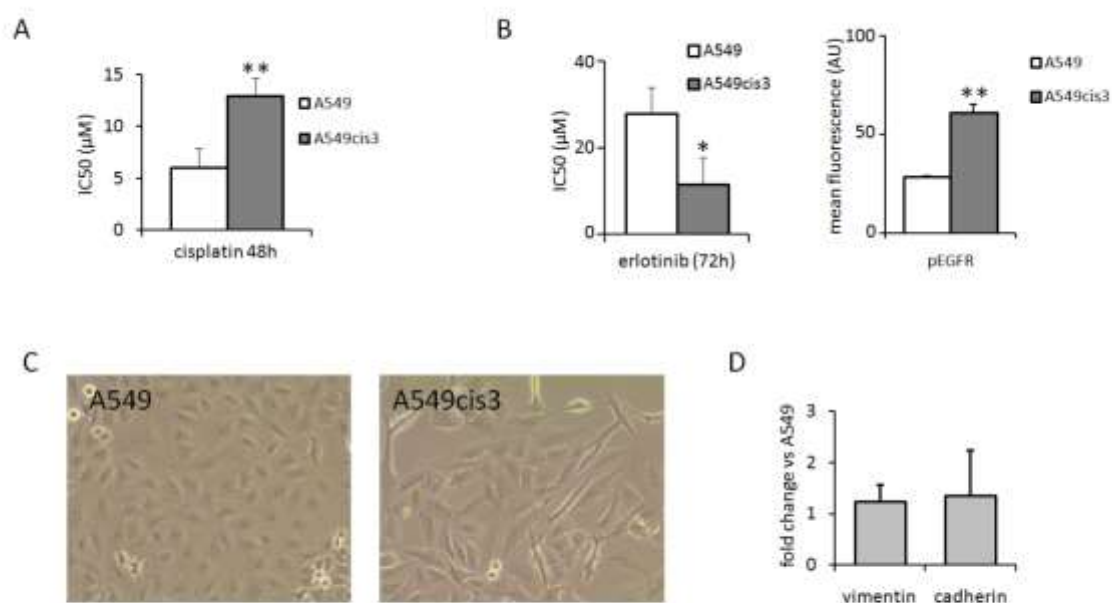

Figure 2

Figure 3: A, Conditioned medium (CM) was prepared from A549 cells treated by cisplatin 3μM 48h or not, or from A549cis3 cells. These media were used to dilute erlotinib for the calculation of A549 naïve cells IC50 to erlotinib 72h in CM as described in figure 2(A). **: p<0.01 Student t-test. B, Naïve A549 cells were incubated overnight in the conditioned medium from A549 cells treated by cisplatin 3μM 48h or not. Cells were fixed and incubated with EGFR and pTyr100 antibodies. Phospho-EGFR was detected by PLA and quantified as in figure 1(D). The graph shown is representative of 5 independent experiments. C, CM was prepared from the three wtEGFR cell lines treated by cisplatin 3μM 48h or not and the indicated compounds were measured by ELISA. Data shown are the mean + SD from 3 independent experiments. **: p<0.01 Student t-test. D, CM were prepared as in C (see material and methods for details); the table summarizes the variation of the indicated compounds concentration in CM and their ability to induce naive A549 cells sensitization to erlotinib. E, A549 cells were treated by cisplatin 3μM 48h or not and then by EGFR blocking antibody 13nM 72h. Cell death was measured by To-Pro3 staining and detected by flow cytometry as in figure 1C. The graph shown is representative of 3 independent experiments.**: p<0.01 Student t-test.
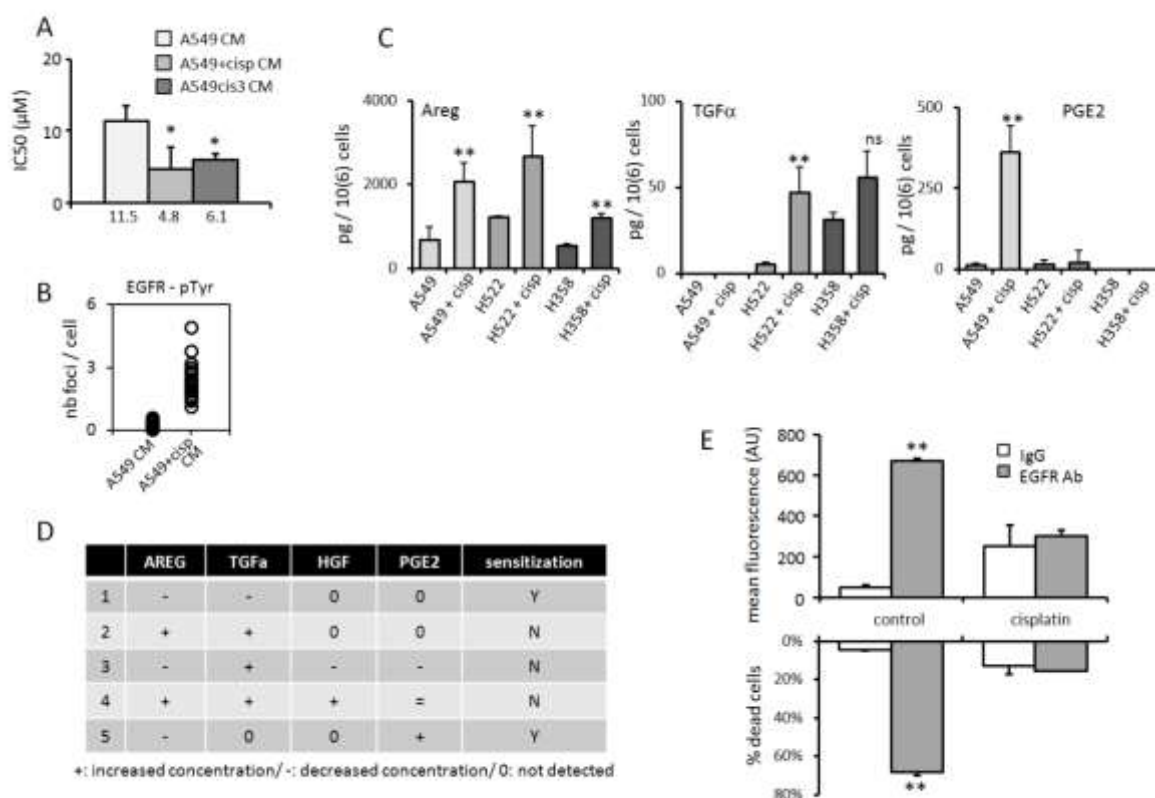

Figure 3

Figure 4: A, A549 cells were treated by the cisplatin - erlotinib (30µM) sequence as described before; when indicated, PP1 (10µM) was added during cisplatin treatment. Cell death was measured by ToPro3 staining and detected by flow cytometry as in figure 1C. The graph shown is representative of 3 independent experiments. **: p<0.01 Student t-test. B, A549 and H1975 cells were treated as in (A) (respectively by erlotinib 30 and 10µM), without (upper graph) or with PP1 (lower graph) added during cisplatin treatment. The graph shown is representative of 3 independent experiments. *: p<0.05 **: p<0.01 Student t-test. C, A549 cells were treated by cisplatin 3µM 48h with PP1 (10µM) added or not. Cells were fixed and stained by pEGFR (pY1068) antibody coupled to a fluorescent secondary antibody and EGFR phosphorylation was detected by flow cytometry. The graph shown is representative of 3 independent experiments. **: p<0.01 Student t-test. D, A549 cells were treated by cisplatin 3µM 48h and IL6 secretion was measured by ELISA in cell supernatants. E, A549 cells were treated as in (A) with IgG or IL6 neutralizing antibody (1µg/ml) added when cisplatin and erlotinib are applied. Cell death was measured by To-Pro3 staining and detected by flow cytometry as in figure 1C. Data shown are the mean + SD from 5 independent experiments. *: p<0.05**: p<0.01 Student t-test.
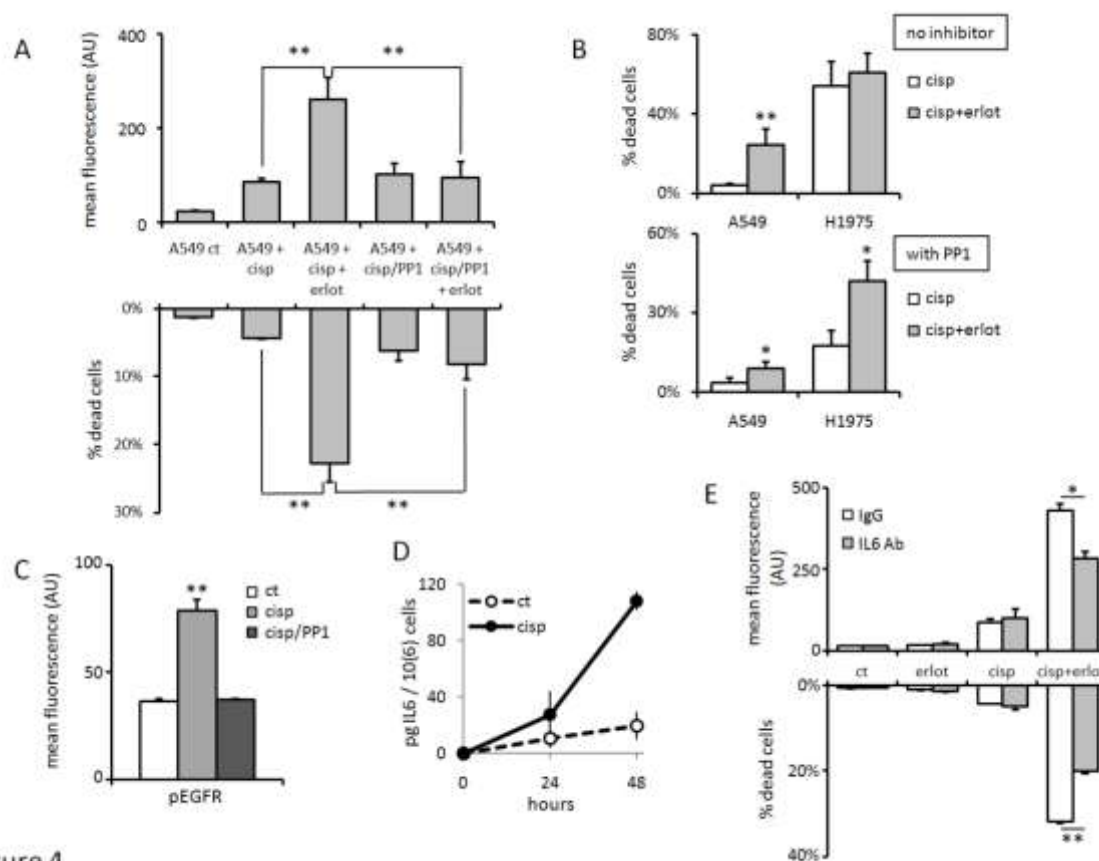

Figure 4

Figure 5: PDXs were grafted to Swiss Nude mice randomly assigned to four groups (PDX A: LCF-04; PDX B: IC14-LC16; PDX C: LCF-09; PDX D: IC8-LC10). Tumor volume was measured twice a week and normalized to the initial volume. Mean relative volume was calculated for each group and represented on the graphs (+/- SD). Student t-test was realized and significant p values between erlotinib and cisplatin/erlotinib groups were indicated on the graphs, provided that no statistical difference exists between control and cisplatin groups at the same time point.(*: p<0.05 **: p<0.01 Student t-test.)
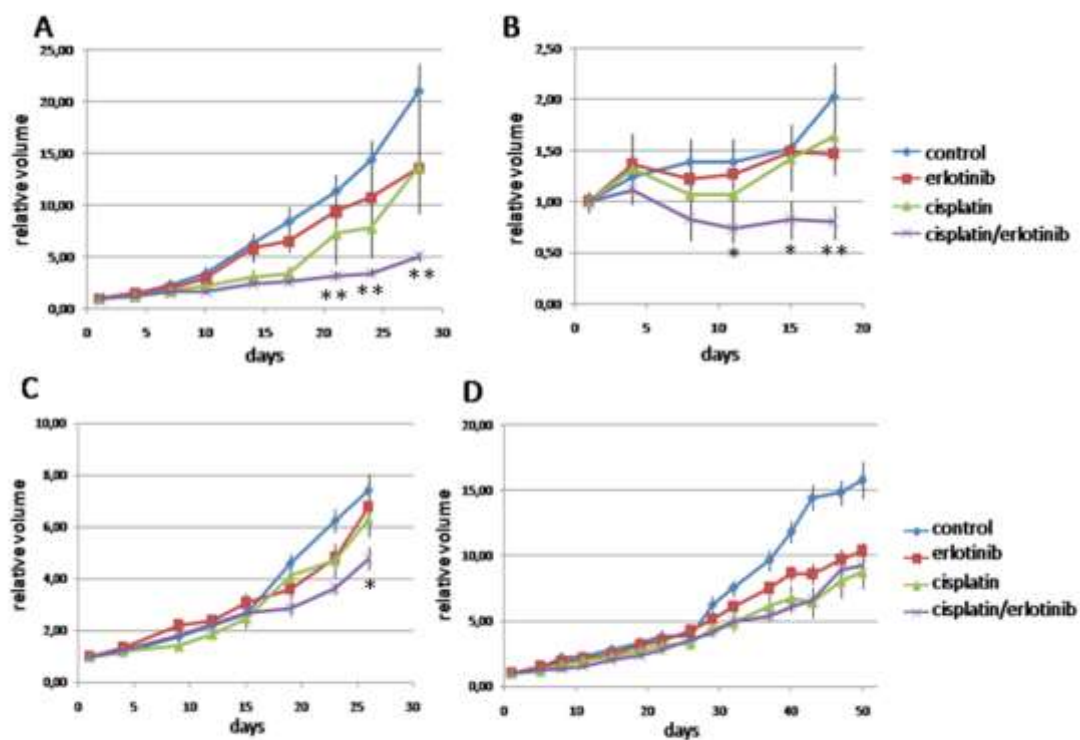

Figure 5

Figure 6: A, IL6, IFIT1 and IFI27 mRNA expression was measured by RT-PCR in A549 cells treated by cisplatin (3µM, 48h) and in A549cis3 cells and expressed as fold change versus control A549 cells. The graph shows the mean + SD from 3 independent experiments. *: p<0.05 (Student t-test). B: The same mRNA measurements were made in PDX A, B and D at day 4 (A4.1 to 3, B4.1 to 3, D4.1 to 3), 8 (A8.1 to 3, B8.1 to 3, D8.1 to 3) and 18 (A18.1 to 3, B18.1 to 3, D18.1 to 3) post-cisplatin injection and expressed as cumulative fold change versus non-treated PDX (A0.1 to 3, B0.1 to 3, D0.1 to 3). C: A principal component analysis was performed with the mRNA as quantitative variables and with response and time categories as qualitative variables.
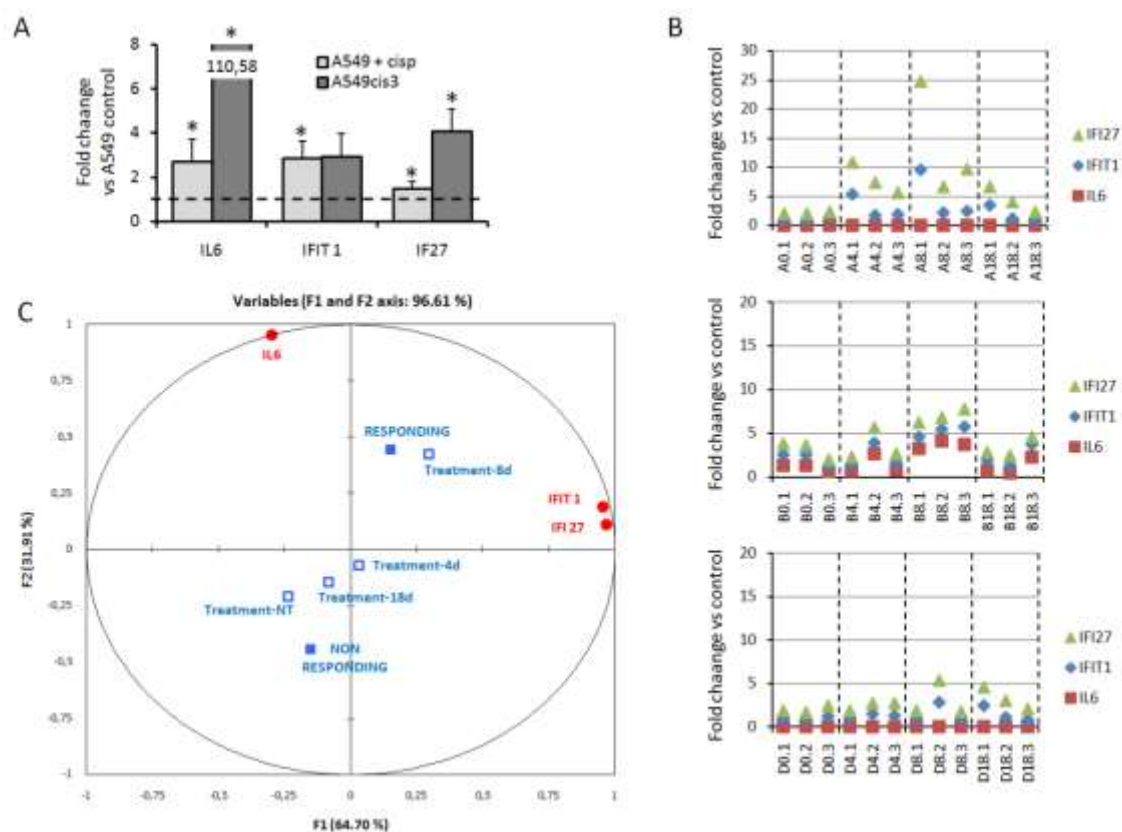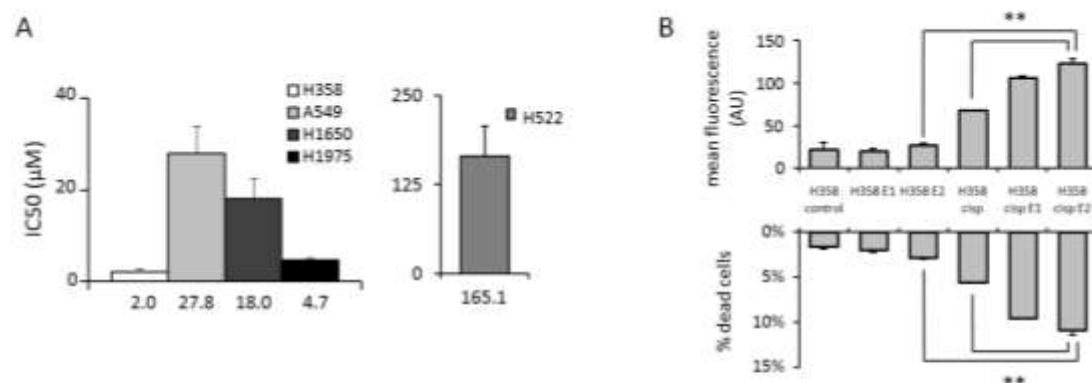

Figure 6

Supplementary data

Figure S1 : A) Cells were treated by a range of erlotinib for 72 hours and IC50 was calculated by the MTT assay according to Chou (2006). B) H358 cells were treated by erlotinib 1 (E1) or 2μM (E2) for 48h following cisplatin pretreatment when indicated (3μM, 48h); cell death was assessed by flow cytometry as described in material and methods. The graph shown is representative of four independent experiments
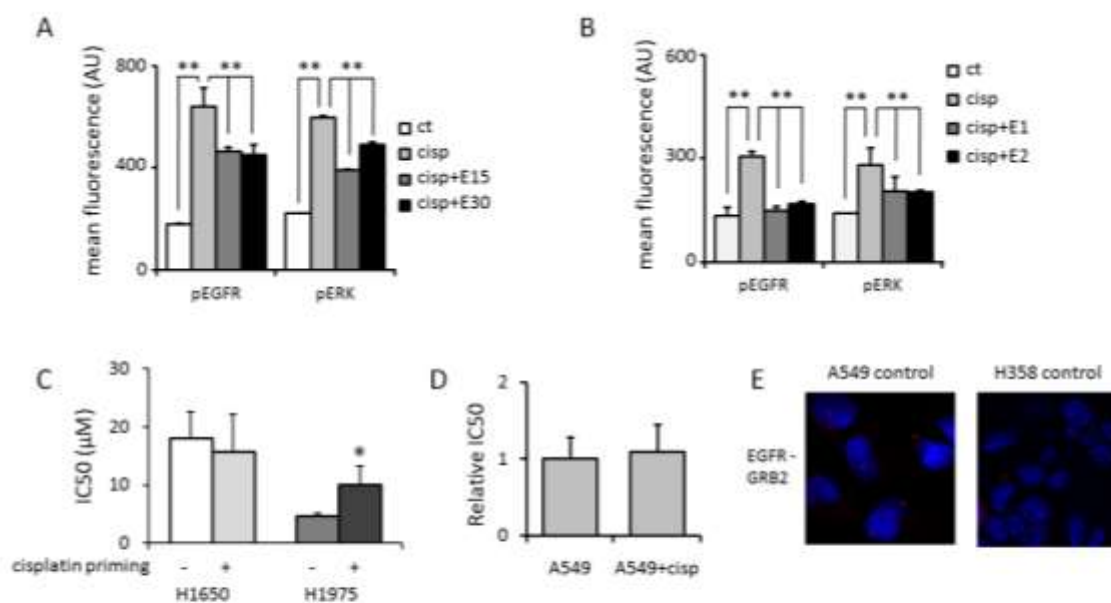

Figure S2 : A549 (A) and H358 (B) cells were treated by cisplatin 3μM 48h (cisp) followed by erlotinib for 72h for the indicated dose (15 or 30μM for A549 cells, 1 or 2μM for H358 cells). Cells were then fixed and incubated with anti-pEGFR (pY1068) or anti-pERK (pT202-pY204). Fluorescence was measured by flow cytometry. C) The IC50 of mutated-EGFR cell lines to erlotinib (72h) was calculated according to Chou et al.(2006) with or without cisplatin priming (3μM, 48h) before elotinib treatment. D) the IC50 of A549 cells to erlotinib was calculated in the absence or presence of cisplatin 3μM for 72h. E) Representative images of EGFR-GRB2 dimerization in control A549 and H358 cells observed by the PLA technique (Blue: DAPI nuclear staining; Red: PLA spots).
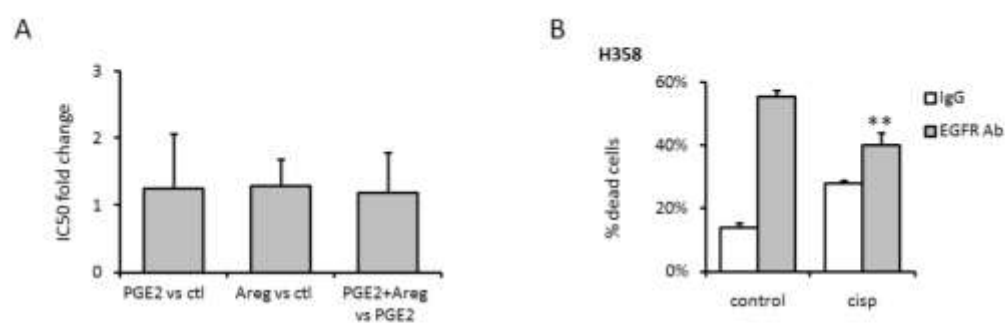
Figure S3 : A) A549 cells were treated by PGE2, amphiregulin or both and the cells IC50 to erlotinib was calculated as described in materials and methods. The mean IC50 fold change (+sd) versus control conditions is represented on the graph. No significant change was observed. B) H358 cells were treated by cisplatin 3μM 48h (cisp) followed by a blocking EGFR antibody for 72h. Cell death was measured by Topro3 staining and detected by flow cytometry.
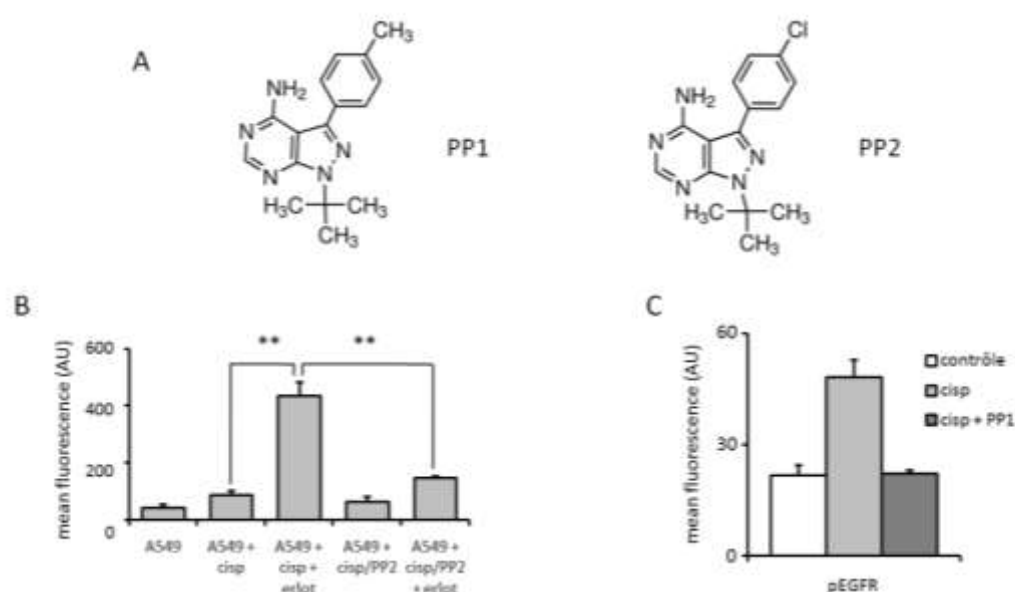

Figure S4 : A) Chemical structure of Src inhibitors PP1 and PP2. B) A549 cells were treated by the sequential treatment cisplatin + erlotinib with or without PP2 added during to cisplatin as described in the manuscript with PP1. Cell death was measured by To-Pro3 staining as desribed in the main text. C) H358 cells were treated by cisplatin 3μM 48h (cisp) +/- PP1 10μM. Cells were fixed and stained with anti pEGFR (Cell Signaling # 3777) coupled to a FITC-labelled secondary antibody as described in material and methods. Fluorescence was detected by flow cytometry.
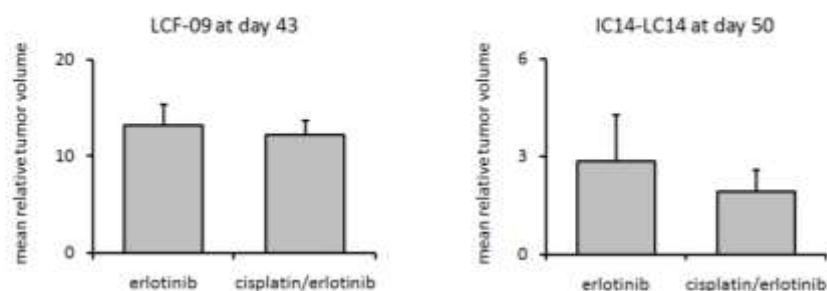
Figure S5: PDX experiments with the indicated tumors were allowed to grow until the benefit from the cisplatin-erlotinib sequential treatment disappeared, providing the tumors did not reach the volume of 2500mm³. The mean (+sd) relative tumor volume in the corresponding mice group is indicated in the graphs. As represented on the graphs, at the indicated time, no significant difference between both groups is observed anymore.
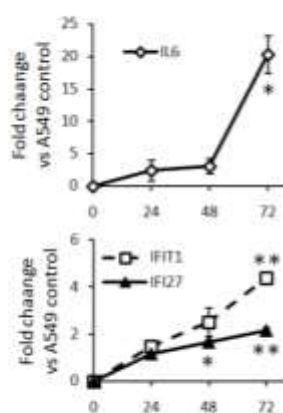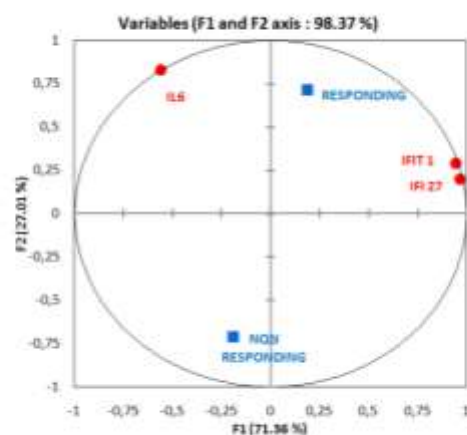
Figure S6 : A) IL6, IFIT1 and IFI27 mRNA were measured from A549 cells treated by cisplatin 3µM at indicated time points and normalized to the corresponding mRNA levels in control A549 cells at the same time points. The measurements were made in duplicate from three independent experiments, the graphs represent mean fold change +/-sd. *: $p<0.05$; **: $p<0.01$ (Student t-test). B) Pearson's principal component analysis (PCA) was made with the Q-PCR analyses from PDXs mRNA at day 8 post-cisplatin treatment. PDX were subclasses into responding (PDX A and B) or non-responding (PDX D) tumors

| Variables	IFIT 1	IFI 27	IL6	Treatment-NT	Treatment-4D	Treatment-8D	Treatment-18D	Responding	Non responding
IFIT 1	1	0,895	-0,111	-0,243	0,008	0,325	-0,091	0,170	-0,170
IFI 27	0,895	1	-0,182	-0,280	0,030	0,369	-0,119	0,256	-0,256
IL6	-0,111	-0,182	1	-0,130	-0,074	0,318	-0,154	0,381	-0,381
Treatment-NT	-0,243	-0,280	-0,130	1	-0,333	-0,333	-0,333	0,000	0,000
Treatment-4D	0,008	0,030	-0,074	-0,333	1	-0,333	-0,333	0,000	0,000
Treatment-8D	0,325	0,369	0,318	-0,333	-0,333	1	-0,333	0,000	0,000
Treatment-18D	-0,091	-0,119	-0,154	-0,333	-0,333	-0,333	1	0,000	0,000
Responding	0,170	0,256	0,381	0,000	0,000	0,000	0,000	1	-1,000
Non responding	-0,170	-0,256	-0,381	0,000	0,000	0,000	0,000	-1,000	1
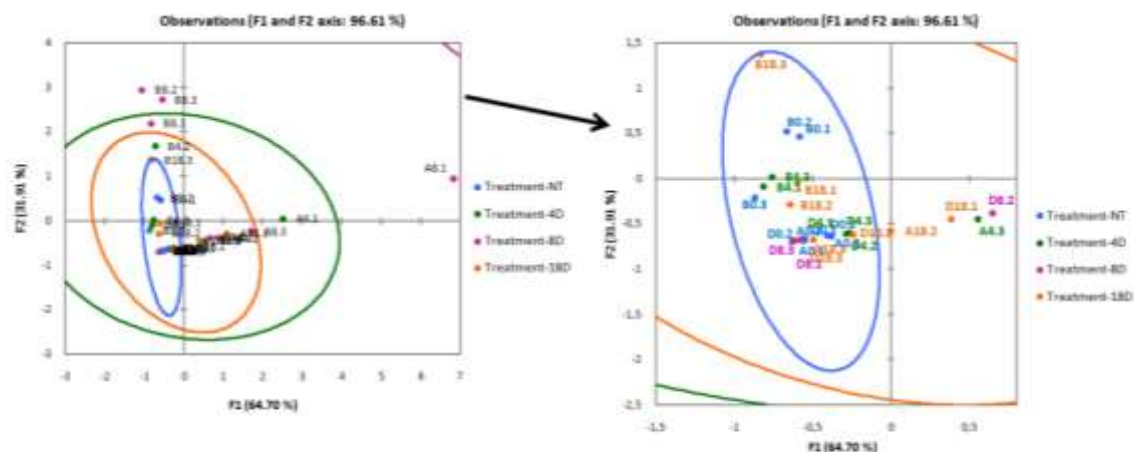
Figure S7 : A) Pearson's correlation matrix attached to the principal component analysis is shown above. Values in bold represent the significative correlation ($p < 0.05$). B) Individual data points are represented on the graph (left) featuring confidence ellipses. The magnification panel on the right indicates that Treatment-8D data points divert from the control ellipse (Treatment-NT ellipse, blue) except from the 8-day PDX D data (D8.1, D8.2 and D8.3).

PDX name	treatment	IFIT1	IL6	IFI 27	response
A	NT-1	0.97	0	0.95	y
	NT-2	0.77	0	1,23	y
	NT-3	1,36	0	0,86	y
	4J-1	5,39	0	5,46	y
	4J-2	1,73	0	5,62	y
	4J-3	1,8	0	3,84	y
	8J-1	9,45	0	15,35	y
	8J-2	2,2	0	4,38	y
	8J-3	2,45	0	7,21	y
	18J-1	3,43	0	3,23	y
	18J-2	1,11	0	2,85	y
	18J-3	0,67	0	1,67	y
B	NT-1	1,29	1,26	1,23	y
	NT-2	1,22	1,34	1,09	y
	NT-3	0,62	0,59	0,74	y
	4J-1	0,73	0,71	0,86	y
	4J-2	1,3	2,64	1,67	y
	4J-3	0,8	0,82	1,04	y
	8J-1	1,33	3,23	1,65	y
	8J-2	1,35	4,11	1,37	y
	8J-3	2	3,73	2	y
	18J-1	1,16	0,69	0,95	y
	18J-2	0,84	0,46	1,16	y
	18J-3	1,41	2,31	0,85	y
D	NT-1	1	0	0,91	n
	NT-2	0,85	0	0,84	n
	NT-3	1,16	0	1,3	n
	4J-1	1,02	0	0,86	n
	4J-2	1,45	0	1,27	n
	4J-3	1,27	0	1,48	n
	8J-1	0,91	0	0,95	n
	8J-2	2,85	0	2,46	n
	8J-3	0,85	0	0,91	n
	18J-1	2,48	0	2,07	n
	18J-2	1,11	0	1,91	n
	18J-3	0,81	0	1,2	n

Table S1: markers quantification by RT-qPCR in the individual mice.